Title
ACTIVE OPTIMIZATION OF THE PERFORMANCE OF A GAS-TURBINE COMBUSTOR

Journal
Combustion Science and Technology, 177(9)

ISSN
0010-2202

Authors
MIYASATO, MM
McDONELL, VG
SAMUELSEN, GS

Publication Date
2005-09-01

DOI
10.1080/00102200590959396

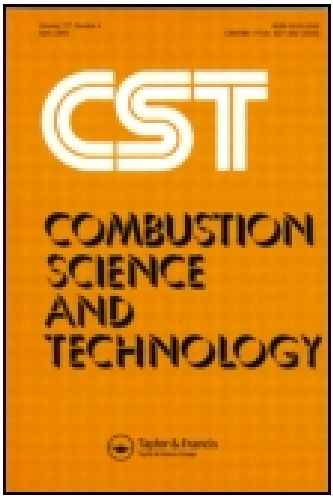

Combustion Science and Technology

Publication details, including instructions for authors and subscription information:
http://www.tandfonline.com/loi/gcst20

ACTIVE OPTIMIZATION OF THE PERFORMANCE OF A GAS-TURBINE COMBUSTOR

M. M. MIYASATO [a] , V. G. McDONELL [a] & G. S. SAMUELSEN [a]

[a] UCI Combustion Laboratory, University of California , Irvine, California, USA

Published online: 30 Aug 2006.

To cite this article: M. M. MIYASATO , V. G. McDONELL & G. S. SAMUELSEN (2005) ACTIVE OPTIMIZATION OF THE PERFORMANCE OF A GAS-TURBINE COMBUSTOR, Combustion Science and Technology, 177:9, 1725-1745, DOI: 10.1080/00102200590959396

To link to this article: http://dx.doi.org/10.1080/00102200590959396

Combust. Sci. and Tech., 177: 1725–1745, 2005

ISSN: 0010-2202 print/1563-521X online
DOI: 10.1080/00102200590959396

Taylor & Francis
Taylor & Francis Group

ACTIVE OPTIMIZATION OF THE PERFORMANCE OF A GAS-TURBINE COMBUSTOR

M. M. MIYASATO
V. G. McDONELL
G. S. SAMUELSEN*

UCI Combustion Laboratory, University of California, Irvine, California, USA

A model natural gas–fired gas-turbine combustor is utilized to evaluate active optimization strategies. Sensors for exhaust species and reaction zone chemiluminescence are utilized with an adaptive fuel injection strategy in a closed-loop feedback control system. The feedback sensors consist of (1) traditional extractive probe-based exhaust measurements of CO and NO_x emissions and (2) chemiluminescence to provide very fast, yet accurate, indicators of performance. A direction-set algorithm is utilized to search for the region of optimal performance. The objectives of the study are to assess (1) the viability of controlling the spatial distribution for performance control; (2) the use of flame chemiluminescence as a fast, inferential emissions sensor for faster feedback; and (3) the robustness of the adaptive control strategy over the entire operability range and under a simulated perturbation mode. For the current study, a

Received 27 October 2004.

The original version of this material was published by the Research and Technology Organization, North Atlantic Treaty Organization in Meeting Proceedings MP-051, "Active Control Technology for Enhanced Performance Operational Capabilities of Military Aircraft, Land Vehicles, and Sea Vehicles," June 2001.

This work was funded in part of the California Energy Commission, California Institute for Energy Efficiency, the U.S. Department of Energy Advanced Turbine Systems program, and the Southern California Gas Company. The efforts of Mr. Steve Hill are greatly appreciated for his assistance throughout the project.

*Address correspondence to gss@uci.edu

simulated injector perturbation scenario (partial fuel-jet blockage) is utilized to examine the robustness of the optimization strategies. The results obtained illustrate the relative correlation of the different sensor strategies with system performance and the ability of the closed-loop control to maintain combustion performance in light of a simulated hardware perturbation.

Keywords: active control, combustor, gas turbine, natural gas, sensor

INTRODUCTION

Due to increasingly stringent emissions regulations for industrial, stationary combustion sources, low-emissions technologies are relying more and more on lean, well-mixed, or premixed strategies. These strategies, although proficient at reducing NO_x emissions, suffer from reduced stability or decreased system efficiency under operating conditions that are often desirable for low emissions; as a result, high-performance operation can present operational and safety challenges. An attractive technology to address these challenges is the application of *active optimization* of the combustion process using feedback sensors, an optimization algorithm, and computer control of the combustor. Major challenges associated with conducting this type of adaptive optimization on industrial combustion systems include identifying (1) parameters amendable for control, (2) reaction characteristics appropriate for feedback sensing, (3) sensor and control time response requirements, and (4) low maintenance and cost impacts. This study investigates the applicability of adaptive fuel injection to stationary gas turbines in relation to these challenges and over several operational scenarios.

Active control of gas turbines has been studied using dynamic control of the fuel injection to offset combustion instabilities (e.g., Lee et al., 1998; Neumeier and Zinn, 1996). An alternative strategy is to tailor the fuel and air mixing to (1) minimize emissions and (2) avoid instabilities; the amount of mixing has been shown to significantly affect the emissions (Appleton and Heywood, 1976; Lyons, 1981) as well as stability (Shih et al., 1996). The research addressed in this paper investigates this latter strategy, that is, to minimize emissions by actively controlling the spatial fuel and air mixedness such that high performance is achieved despite changes in load (equivalence ratio) or hardware degradation.

Toward this end, a novel fuel injection strategy is applied to provide sufficient, flexible, and simple control over the entire turndown or duty cycle range of the gas turbine. The active optimization strategy is tested over the stability range of the combustor and then tested under a simulated hardware degradation or unexpected perturbation mode, where two injector fuel jets are partially blocked.

To respond rapidly to unexpected changes, fast feedback sensors are required. Previous work identified the need for such feedback control to attain and maintain high performance under changing load conditions (Davis and Samuelsen, 1996; Docquier and Candel, 2002; Jackson and Agrawal, 1999; St. John and Samuelsen, 1994). These fast sensors would be situated near the reaction, thereby avoiding the long convection times associated with exhaust sampling, and would therefore provide faster optimization reduced emissions even during load cycling, and, if possible, stability information. These feedback sensors will most likely be optical to provide the fast time response required (e.g., Najm et al., 1998). Of particular interest would be a direct inference of emissions behavior and stability with a single sensor system. As a first step toward this goal, the ability of flame chemiluminescence to accurately reflect the emissions performance is assessed.

OBJECTIVES AND APPROACH

The objectives of the current study are to assess the viability and degree of success of (1) flexible spatial mixing strategy for performance control, (2) the use of flame chemiluminescence as a fast, inferential emissions sensor for faster feedback, and (3) the robustness of the adaptive control strategy over the entire operability range and under a simulated perturbation mode.

A four-step approach was utilized in the current study:

1. Measure the NO_x, CO, and chemiluminescence emissions over the entire operability range of the model combustor.
2. Identify the regions of optimal performance (in terms of low NO_x and CO).
3. Apply and compare active control to the conventional emissions analyzers using the chemiluminescence sensor.
4. Simulate a hardware perturbation by blocking two injector jets and apply active control to assess the systems response.

EXPERIMENT

The test facility provides a wide range of operating conditions and flow metering. The test stand is designed to operate at 1 atm with inlet temperatures up to 800 K. The model combustor test rig, shown in Figure 1, has a quartz liner to allow optical access for reaction visualization and chemiluminescence measurements.

Model Combustor

The model combustor utilizes two independent natural gas injection circuits to tailor to the fuel distribution. The first fuel circuit injects the fuel radially from the centerbody into the swirling airstream. This centerbody injection circuit, labeled CB in Figure 2, consists of six equally spaced fuel holes located circumferentially along the side of the fuel manifold. The fuel manifold is positioned directly above the swirler hub. The second fuel injection circuit allows fuel to be injected radially inward from the surrounding wall. This wall injection circuit, labeled WJ in Figure 2, consists of six equally spaced fuel holes in positions that are staggered with respect to the centerbody injection holes. By varying the fuel split between the two fuel circuits, a variety of fuel distributions can be achieved, as described in detail by Flores et al. (2000).

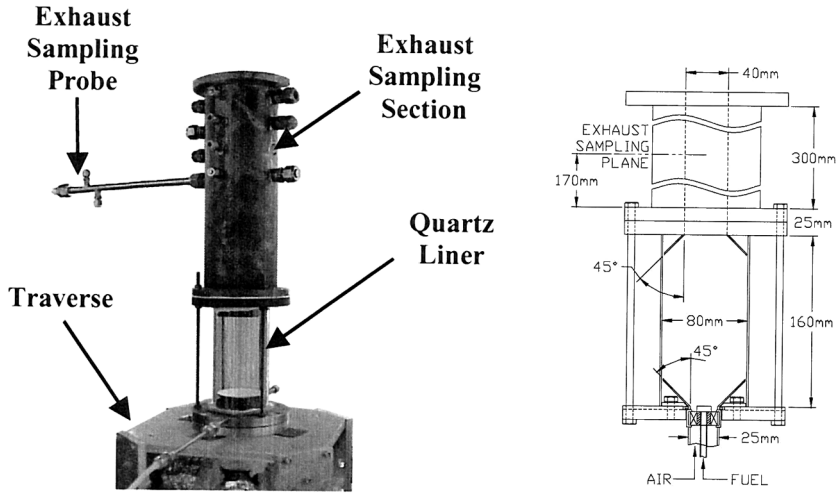

Figure 1. Test facility.

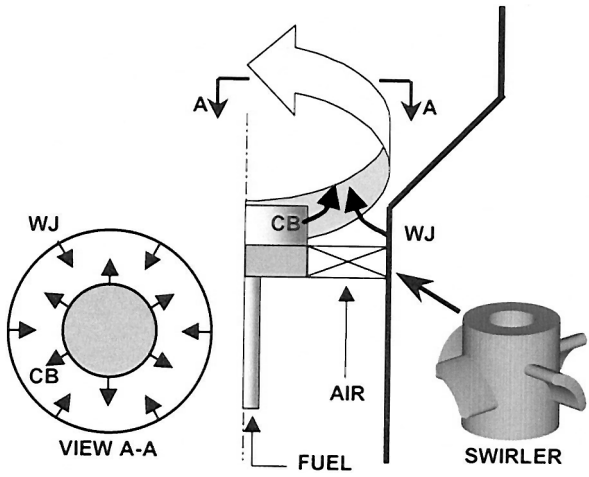

Figure 2. Detail of fuel injection options.

The baseline configuration is a four-vane axial swirler. The nominal firing rate for the system is 15 kW of natural gas at 0.0093 kg/s of air, although the fuel flow rates were varied to assess the system's performance. An air inlet temperature of 700 K was utilized in all cases.

Diagnostics

Because the general objective of the optimization strategy is to mitigate exhaust gas pollutants, a direct measure of the pollutants is warranted. Exhaust emissions were collected via a 12.7-mm-diameter, water-cooled, stainless steel extractive probe. This emissions probe is used to sample the exhaust emissions downstream of the exit plane of the combustor, as shown in Figure 1. This probe is designed to take an integrated average measurement of the emissions over the diameter of the sampling plane. The water in the probe is heated to 325 K to protect the probe and quench the sample while avoiding condensation of water vapor inside the probe. The emissions are pumped through a heated Teflon line to prevent water condensation. The sample stream goes through a converter to reduce any NO_2 to NO prior to the water dropout. After the water dropout, the exhaust gas is delivered to a portable emissions analyzer (Horiba Ltd. Model PG250A), which measures carbon monoxide (CO), carbon dioxide $(CO)_2$ oxygen (O_2), oxygen (O_2), and nitrogen oxides (NO_x).

Although the measurement of the combustor exhaust emissions provides a direct indication of the performance, a more convenient strategy with much faster time response is desirable, and likely necessary, to optimize performance and maintain stable combustion. An optimization strategy based on an indirect measure must then estimate the associated combustion performance. Two strategies were investigated: acoustics and reaction chemiluminescence. Although the acoustic measurements yielded some potentially useful results, they were not very robust the additional work is required to attain the desired performance. As a result, only the result from the chemiluminescence investigations are presented here. Chemiluminescence has been widely utilized as an indicator of combustion behavior (e.g., Docquier and Candel, 2002; Lee et al., 2003; Samaneigo, Egolfopoulos, and Bowman, 1995). For the chemiluminescence detection for the present application, three radial species were considered: OH, CH, and CO_2^*. Initial studies were conducted using a polychrometer, and the overall signal levels associated with the CO_2^* chemiluminescence were found to be much greater than those for OH or CH. As a result, the detailed characterizations were conducted using CO_2^*. Details associated with the chemiluminescence of CO_2^* and its interpretation relative to combustion heat release and effects of dilution, strain rate, and other phenomena are described by Samaneigo et al. (1995).

The basic setup for the chemiluminescence utilized a 200-μm core fiber located approximately 49 cm away from the combustor to allow the 14° expansion of the fiber to encompass the entire reaction volume. The fiber end is attached to a collimating lens, which directs the signal through an appropriate filter and then to a photomultiplier tube. In the case of CO_2^*, a 310–600-nm bandpass filter is utilized to capture the CO_2 continuum. For the system studied, the CO_2^* chemiluminescence,

$$CO + O \longrightarrow CO_2^*$$

provided an intense and measurable signal over the entire operability range of the combustor. The data values are sampled at a rate of 25,000 Hz over 3 s. The chemiluminescence has the other obvious advantage that it could potentially be utilized as an instantaneous reaction monitor, thereby providing an indication of the reaction stability. In this case, additional sampling issues must be addressed.

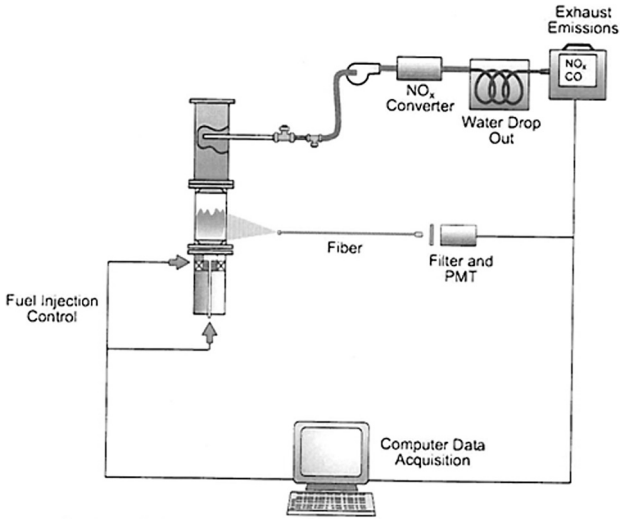

Figure 3. Model gas-turbine diagnostics and control setup.

The basic setup for the direct emissions and chemiluminescence setup is shown schematically in Figure 3. As a result, both direct and estimated performances are determined for the combustor.

Active Optimization

The active optimization strategy utilizes a simple hill climbing, or direction-set, methodology for the search algorithm while trying to continually increase or optimize performance in terms of NO_x and CO emissions. To quantify performance and deal objectively with the trade-off that often occurs between NO_x and CO, a cost function is defined:

$$J = w_{NO_x} \cdot f(NO_x) + w_{CO} \cdot g(CO)$$

where w_{NO_x} and w_{CO} are weighting functions. The definitions and plots of the functions $f(NO_x)$ and $g(CO)$ are

$$f(NO)_x = \begin{cases} 1 - 0.75 \cdot \left(\dfrac{[NO_x]}{5}\right)^4 & [NO_x] \le 5\,\text{ppm} \\ (1 - 0.75) \cdot \dfrac{[NO_x]_{max} - [NO_x]}{[NO_x]_{max} - 5} & [NO_x] > 5\,\text{ppm} \end{cases}$$

$$g(\mathrm{CO}) = \begin{cases} 1 - 0.90 \cdot \left(\dfrac{[\mathrm{CO}]}{8}\right)^4 & [\mathrm{CO}] \le 8\,\mathrm{ppm} \\ (1 - 0.90) \cdot \dfrac{[\mathrm{CO}]_{\max} - [\mathrm{CO}]}{[\mathrm{CO}]_{\max} - 8} & [\mathrm{CO}] > 8\,\mathrm{ppm} \end{cases}$$

The performance, J, therefore increases with decreasing NO_x and CO (i.e., good performance).

The search algorithm uses the performance index to comparatively seek out conditions of higher performance. The algorithm controls the combustor by varying the two fuel inputs (centerbody and wall jets) to affect the fuel split and equivalence ratio. The feedback sensors provide the information necessary to calculate the performance parameter J at each condition. The algorithm proceeds along a certain direction until J is not longer maximized. The algorithm then simply chooses a new direction at a predetermined angle and step size. If the new condition has a higher performance index, then the algorithm proceeds in the new direction; if the performance is not higher, another new angle of rotation is selected, and so on. For the present study, the functions of NO_x and CO are equally weighted.

RESULTS

Baseline Configuration

To establish the research baseline and know whether the active optimization was successful, exhaust emissions and chemiluminescence measurements were taken over the model combustor's entire operational space. Furthermore, to facilitate a most direct interpretation of the optical measurements, CO_2^* chemiluminescence measurements were compared and correlated with the exhaust emissions. The average CO_2^* signal was found to correlate with the exhaust NO_x concentration, and the percent fluctuating CO_2^* signal to the exhaust CO emissions (Figure 4). This correlation allows a direct determination of the combustion performance to be performed in a manner that was consistent with the approach used for the exhaust emissions. It is noted that this particular combustor configuration did not exhibit strong combustion oscillations (e.g., pressure fluctuations were generally less than 1% of the mean pressure level). It is possible that higher fluctuation levels would result in a correlation that is less significant.

a) NOx vs. Average Chemiluminescence Signal

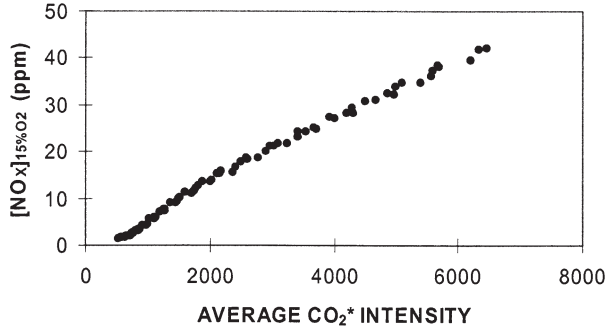

b) CO vs. % Fluctuation of Chemiluminescence

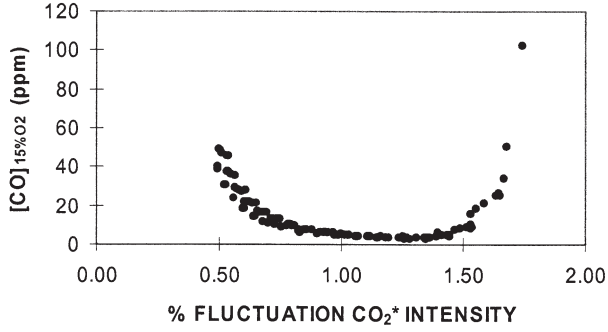

Figure 4. Exhaust emissions correlation with chemiluminescence.

The NO_x and CO emissions were then used to calculate performance J, as described previously. The resulting performance map is shown in Figure 5 in the form of a contour map of the performance as a function of equivalence ratio and fuel split. (In all of the subsequent similar figures, the y axis represents the fuel split as a percentage of fuel injected through the centerbody jets and the x axis represents the equivalence ratio.) The region of peak performance is located in the ridge along the 0.42 equivalence ratio and between fuel splits from 20 to 60%. The plot shows that the performance is relatively insensitive to the fuel split, giving rise to the large region of high performance (i.e., $J = 0.9$) at the 0.42 equivalence ratio. As a result, the operation of the combustor

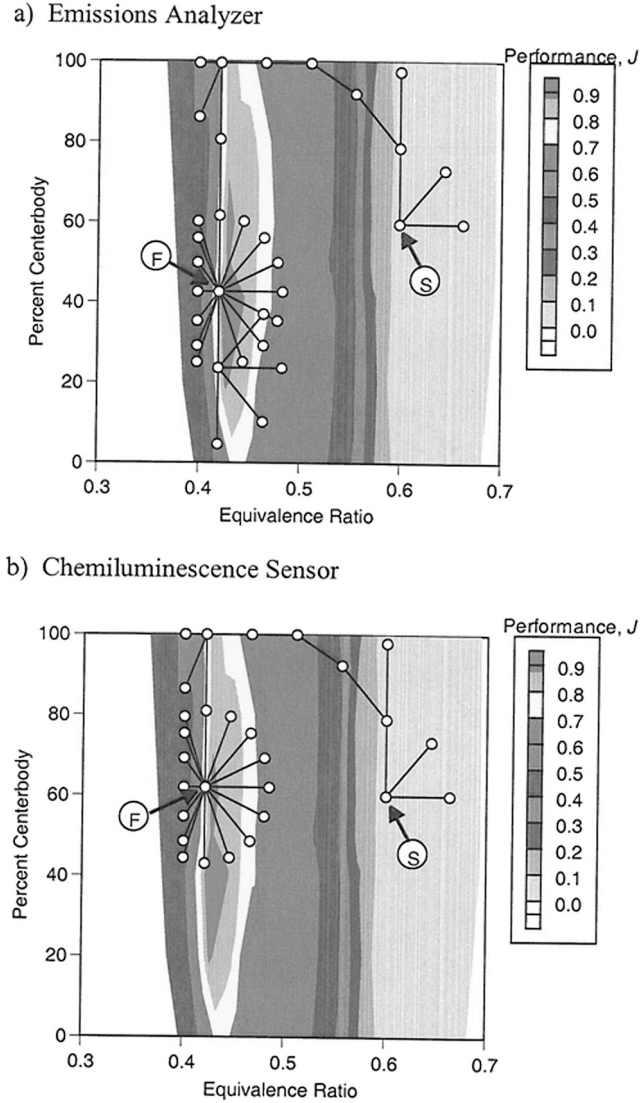

Figure 5. Performance map for model gas-turbine combustor and active optimization history.

at this equivalence ratio for fuel splits between about 20 and 70% would provide optimal performance. Any optimization algorithm should therefore drive the combustor operation to this region.

The active optimization control system was applied to the model combustor using the exhaust emissions analyzers as the feedback sensor. The resulting search path is shown overlaid on the performance map in Figure 5*a*. The combustor was started at an arbitrary poor performing condition and allowed to optimize, finishing very near the absolute peak performance condition. The search took 21 iterations and 28 min to settle on the optimum ridge.

Based on the correlations shown in Figure 4, the optimization process was revisited with the chemiluminescence-based feedback (i.e., estimation) for performance incorporated into the active optimization system. The resulting search is shown in Figure 5*b*. Although the chemiluminescence feedback optimized on a slightly different fuel split than the emissions feedback, the difference in performance index is only about 0.002. Furthermore, the chemiluminescence was able to optimize at a much faster rate: four times faster than the emissions feedback case. In fact, the response of the sensor was sufficient to allow even faster optimization; however, the time constant associated with the overall system establishes a reasonable limit. Indeed, this aspect of the system dynamic control for optimization of performance requires careful consideration in the development of actuation and control algorithms. If the controller is too aggressive, damage may result.

As shown in Figure 5, the active optimization strategy of using flexible fuel injection and two different feedback sensors (emission analyzers and reaction chemiluminescence) was able to successfully identify the regions of highest performance, with the chemiluminescence feedback offering much faster time response. The next test was to determine the robustness of the system by applying a large change to the system hardware.

Partially Blocked Injector

To provide a scenario with which to evaluate the utility of the sensor and optimization strategies, the fuel injector was perturbed by partially blocking two adjacent centerbody fuel injection jets. In practice, such wear and tear may occur gradually, or, in the case of the ingestion of a foreign object, a rather sudden obstruction may occur. Also, real-time improvement is envisioned for scenarios where fuel compositional changes may occur and lead to variation in performance (e.g., Flores et al., 2000). As an ''extreme'' case of the present evaluation, the partially blocked injector scenario was utilized to provide a significant change in

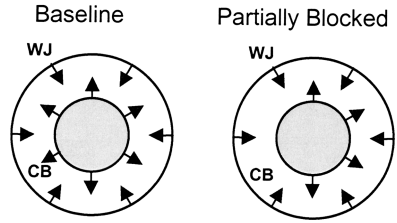

Figure 6. Partially blocked centerbody.

performance. Figure 6 illustrates the strategy utilized in the partial blocking. Basically, two adjacent fuel holes on the centerbody were partially blocked. This asymmetrical blockage resulted in an altered reaction structure compared to the baseline configuration as shown in Figure 7.

a) Baseline Injector

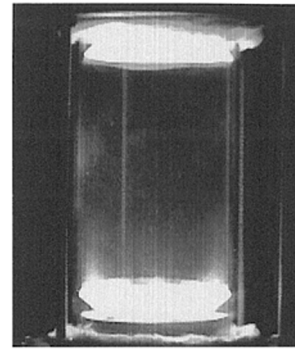

b) Partially Blocked Injector

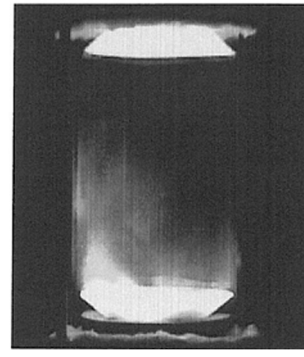

Figure 7. Reaction structures at CB = 60%, $\phi = 0.60$.

The difference in centerbody injector pressure drop causes more fuel injection and higher temperature along the left side of the liner.

To illustrate the impact the partially blocked injector has on the fuel distribution, Figure 8 presents contours of the spatial distribution of fuel measured immediately downstream of the centerbody (see Figure 2). The fuel distributions were measured using a 0.125-in. o.d. sampling probe

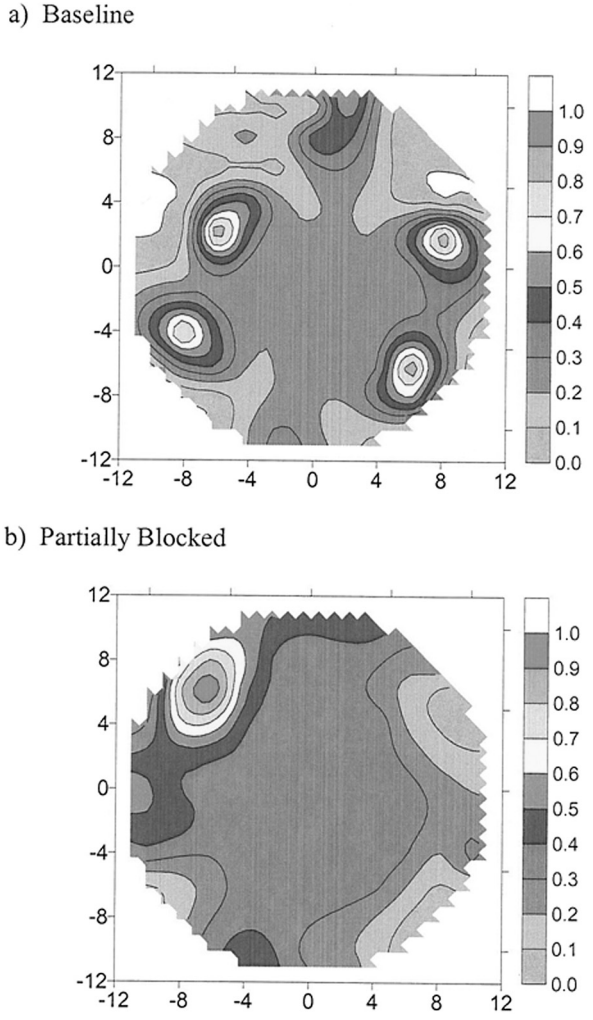

Figure 8. Fuel distribution 3 mm downstream of centerbody.

and a high-range flame ionization detector. Samples were obtained at 131 points over the plane of interest to generate the contour plots shown. The results presented are normalized relative to the maximum fuel concentration measured for each case to highlight the patterns (for more details see Flores et al., 2000). Figure 8*a* reveals that the baseline case exhibits periodic peaks in fuel concentration due to the discrete jets. The apparent asymmetry shown in the baseline case is associated with the location of the fuel jet and the orientation of the axial swirler. The behavior of the fuel jet depends on the relative wake effect behind the four vanes (Flores et al., 2000). In the case of the partially blocked injector, shown in Figure 8*b*, the fuel distribution is clearly skewed to one side of the combustor. In this case, the variation associated with vane wakes appears to be overshadowed by the local increase in fuel due to the two partially blocked holes. Given the rather significant impact on the fuel distribution, the visible reaction structure changes shown in Figure 7 appear relatively minor. As a result of the partial blockage, some performance changes were expected. The resulting performance map is shown in Figure 9 and does indeed show major changes. Again, the change in performance are significant given the relatively minor visible differences in reaction structure shown in Figure 7.

The performance contour plot shown a "valley" at high centerbody fuel ratios. This result is due to the asymmetric centerbody fuel injection and the resulting higher NO_x levels. The optimum conditions subsequently occur at higher wall jet ratios but at the same equivalence ratio (0.42) as in the baseline, unblocked case. The maximum performance values, however, are less than for the unblocked condition. Nevertheless, the active optimization strategy was initiated on this hardware configuration, starting at the optimized condition for the baseline case. This scenario represents an unexpected hardware perturbation from sudden hardware failure or the ingestion of a forgeign object inside the combustor.

The active optimization histories using the emissions feedback and CO_2^* chemiluminescence are shown in Figure 9. The search paths for both optimizations are identical but the chemiluminescence feedback is able to optimize 2.7 times faster than when using emissions feedback.

Thus, the active optimization strategy using the flexible fuel injection and either emissions or chemiluminescence feedback was successful in locating the maximum performance conditions even under degenerated hardware configurations. The chemiluminescence feedback, as in the baseline configuration, provided much faster response and optimazation.

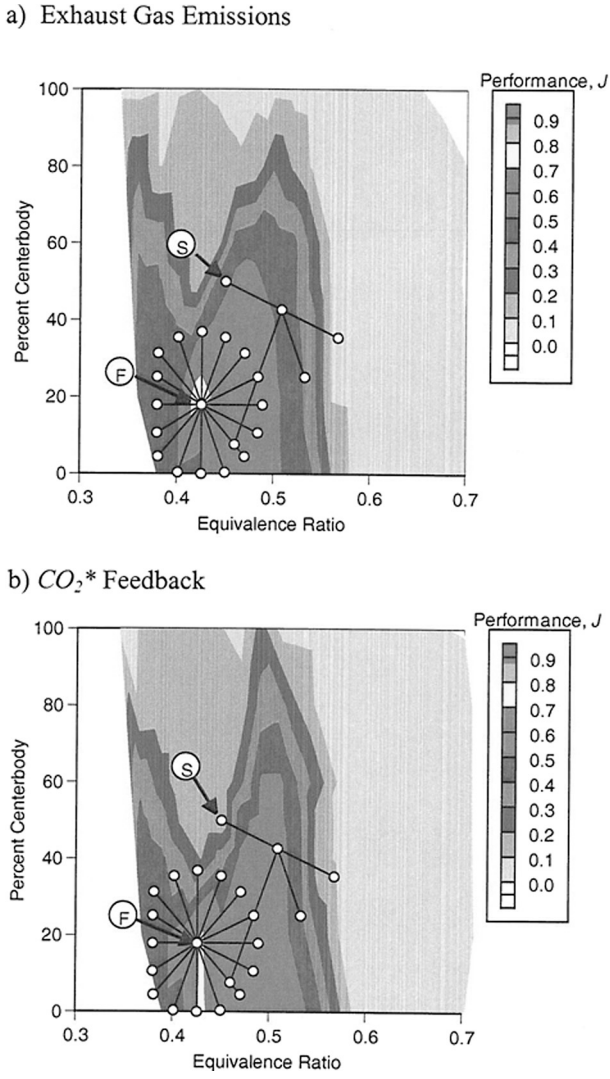

Figure 9. Performance map and optimization history for partially blocked injector.

It should be noted that the performance contour plot illustrated for the chemiluminescence feedback, Figure 9*b*, represents the *inferred* performance based on the chemiluminescence values. Although careful curve fits were conducted for multiple fuel splits for the range of

equivalence ratios, some scatter in the data resulted in differences between the inferred performance (Figure 9*b*) and the emissions-based performance (Figure 9*a*). These differences and their implications are addressed further in the following section.

DISCUSSION

Although not illustrated previously, the different between the actual performance (NO_x and CO emissions) and the inferred measurement (CO_2^* chemiluminescence) can obviously affect the optimization results. The correlations used in the previous optimizations were known a priori from detailed measurements. For practical purposes, it would be desirable to have a general sensor that can determine performance in the absence of a priori knowledge. Figure 10 presents the correlations between the chemiluminescence and the gaseous emissions. In contrast to Figure 4, more scatter is observed in Figure 10. This could be due to a variety of factors, including the condition of the quartz and the relative asymmetry associated with the reaction generated by the partially blocked injector. As a result, despite the apparently robust relationship between the emissions and the chemiluminescence shown for the baseline, the relationship does not hold up in general for the current optical setup and combustor configuration. Note that the NO_x correlation appears to be less sensitive that the CO correlation. It could be argued that chemiluminescence levels should be greater as temperature (and, as a result, NO_x) increases. Hence, the generally well-behaved NO_x response might be expected. CO, on the other hand, has no expected relationship to the chemiluminescence. The fluctuating chemiluminescence intensity may be related to packets of reaction that are quenched as lean blowoff approaches. However, other CO formation scenarios can occur on the lean side and a trade-off of mechanisms is what gives rise to the scatter shown in Figure 10*b*. The results do show promise for the use of fluctuating chemiluminescence for stability, which has been utilized in studies looking at combustion dynamics (e.g., Docquier and Candel, 2002). Additional efforts are under way to look at the optimal location for the sensors as well as others aspects of the chemiluminescence that may allow it to be used in the absence of a priori knowledge of the system behavior in terms of emissions performance.

Even if a priori knowledge is available, the sensitivity of the strategy must be considered. If coarser (i.e., less refined) correlations were used,

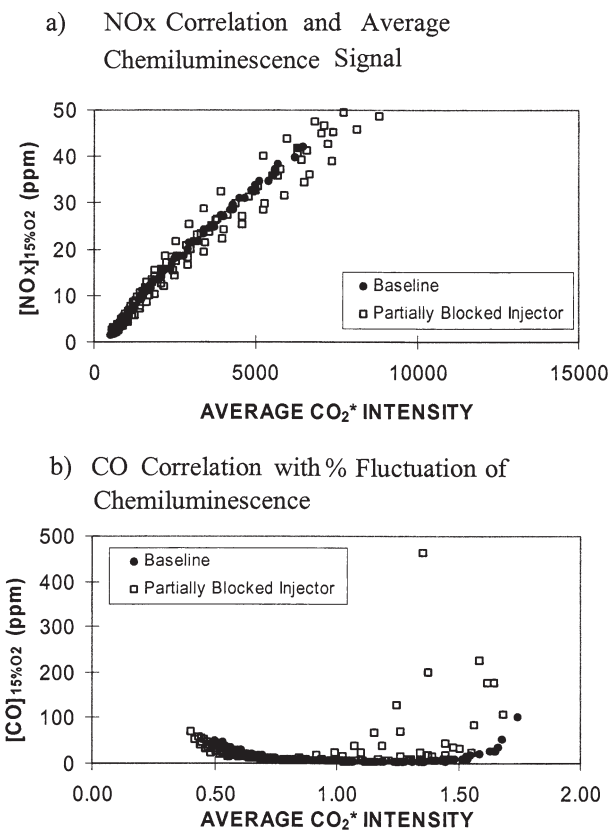

Figure 10. Total chemiluminescence/emissions correlation.

one wonders if the control scheme would still be able to locate the optimum regions, especially if the search (i.e., operational) space is not well behaved, as with the hardware perturbation case. Further questions arise regarding the dependency of the optimization scheme to the initial condition and input search parameters (starting angle, increment angel, and step size). To begin addressing these question, the following parameters were changed for the hardware perturbation configuration:

- starting location,
- starting direction, and
- CO_2^* correlations.

Table 1. Sensitivity assessment

Parameter change	Findings	Implications	Search history
Starting condition: Placed in region far from optimum in poorly performing "valley"	Emissions feedback, located optimum region	Success dependent on algorithm and initial parameters; also emissions feedback is lengthy process	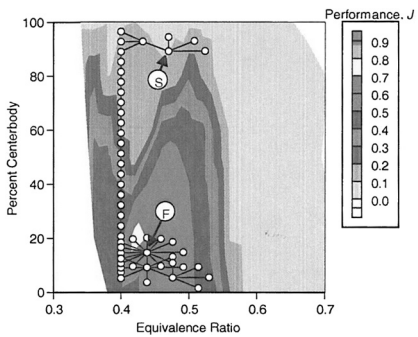
Initial direction: Initial angle pointed in worsening direction	Emissions feedback (not shown), located optimum region CO_2^* feedback (shown) optimized on a local peak and "missed" higher performance region	Common detriment to direction-set algorithm Altering step size would increase chances of "hitting" on peak region Inaccurate CO_2^* correlation to local peak optimization	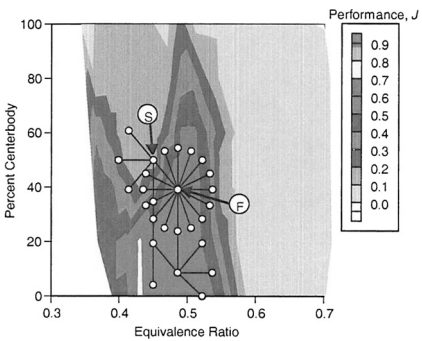

Correlation accuracy: Coarser correlations used to derive NO_x and CO from CO_2^* chemiluminescence	CO_2^* feedback located the optimum region in twelve iterations, but took a greater number of iterations to arrive at a peak	Inferential methods may not need high accuracy but must accurately reflect the performance trends	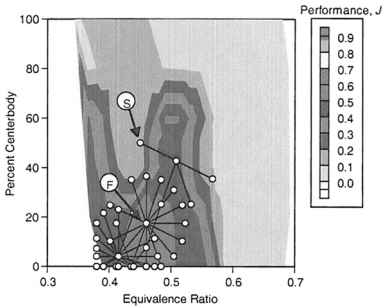
Correlation accuracy and initial direction: Coarser correlations and initial angle pointing in worsening direction	CO_2^* feedback located optimum region	No stability parameter was included, which may have altered search path away from lean limit	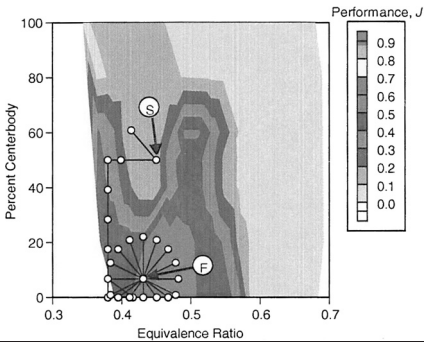

The results of these tests are summarized in Table 1. In each case, the region of optimum performance was located successfully with the algorithm utilized.

CONCLUSIONS

The following conclusions are offered regarding this work:

- The flexible centerbody and wall-jet fuel injection strategy is able to alter mixing and thereby attain and maintain optimal performance for a given equivalence ratio.
- The chemiluminescence sensor provides up to 2.7 times faster feedback and, therefore, allows faster optimization of the system performance.

– The optimization, however, is dependent on the accuracy of inferential sensor correlations to characterize the actual performance parameters of NO_x and CO.
– NOx appears to be robustly correlated to chemiluminescence, whereas CO is not.
– Examples are provided where coarse and fine correlations allow optimization in the correct regions. Care must be taken to accurately reflect the actual parameters of interest, and developing these without a priori knowledge will be challenging.
– The active optimization strategy is able to locate the high-performance region of the model combustor for both the baseline firing configuration and the hardware perturbation scenario, which simulates extreme degradation or ingestion of a foreign body.
– The direction-set search algorithm employed for these initial tests is subject to many pitfalls depending on the initial search parameters (initial direction, step size, etc.) and the contours of the search space (unimodal, bimodal, etc.).
– A stability sensor is required to allow fast, confident, and safe optimization.
– More effort is required to establish a robust correlation between inferential sensors and exhaust gas composition.

REFERENCES

Appleton, J.P. and Heywood, J.B. (1976) The Effects of Imperfect Fuel–Air Mixing in a Burner on no Formation from Nitrogen in the Air and the Fuel, *Proc. Combust. Instit.*, **14**, 777–786.

Davis, N.T. and Samuelsen, G.S. (1996) Optimization of Gas Turbine Combustor Performance throughout the Duty Cycle, *Proc. Combust. Instit.*, **26**, 2819–2825.

Docquier, N. and Candel, S. (2002) Combustion control and sensors: A review. *Prog. Energ. Combust. Sci.*, **28**, 107–150.

Flores, R.M., Miyasato, M.M., McDonell, V.G., and Samuelsen, G.S. (2000) Response of a model gas turbine combustor to variation in gaseous fuel composition. *J. Eng. Gas Turb. Power*, **123**, 824–831.

Jackson, M.D. and Agrawal, A.K. (1999) Active control of combustion for optimal performance. *J. Eng. Gas Turb. Power*, **121**, 437–443.

Lee, J.G., Hong, B.S., Kim, Yang, K.V., and Santavicca, D. (1998) Optimization of Active Control Systems for Suppressing Combustion Instability. *Symposium on Gas Turbine Engine Combustion, Emission, and Alternative Fuels*, RTO—Applied Vehicle Technology Panel, Lisbon.

Lyons, V. (1981) Fuel/air nonuniformity–Effect on nitric oxide emissions. *AIAA J.*, **20**, 660–665.

Najm, H.N., Knio, O.M., Paul, P.H, and Wyckoff, P.S. (1998) A study of flame observables in premixed methane—air flames. *Combust. Sci. Technol.*, **140**, 369.

Neumeier, Y. and Zinn, B.T. (1996) Experimental Demonstration of Active Control Combustion Instabilities Using Real-Time Modes Observation and Secondary Fuel Injection, *Proc. Combust. Instit.*, **26**, 2811–2818.

Samaniego, J.-M., Egolfopoulos, F.N., and Bowman, C.T. (1995) CO_2^* chemiluminescense in premixed flames. *Combust. Sci. Technol.*, **109**, 183–203.

Shih, W.P., Lee, H.G., and Santavicca, D.A. (1996) Stability and Emissions Characteristics of a Lean Premixed Gas Turbine Combustor, *Proc. Combust. Instit.*, **26**, 2771–2778.

St. John, D. and Samuelsen, G.S. (1994) Active, Optimal Control of a Model, Natural Gas-Fired Industrial Burner, *Proc. Combust. Instit.*, **25**, 307–316.